Structures of Si and Ge Nanowires in the Subnanometer Range

R. Kagimura, R. W. Nunes, and H. Chacham*

Departamento de Física, ICEX, Universidade Federal de Minas Gerais, CP 702, 31270-901, Belo Horizonte, Minas Gerais, Brazil

(Received 23 July 2004; published 7 September 2005)

We report an *ab initio* investigation of several structures of pristine Si and Ge nanowires with diameters between 0.5 and 2.0 nm. We consider nanowires based on the diamond structure, high-density bulk structures, and fullerenelike structures. Our calculations indicate a transition from sp^3 geometries to structures with higher coordination, for diameters below 1.4 nm. We find that diamond-structure nanowires are unstable for diameters smaller than 1 nm, undergoing considerable structural transformations towards amorphouslike wires. For diameters between 0.8 and 1 nm, filled-fullerene wires are the most stable. For even smaller diameters ($\sim$0.5 nm), we find that a simple hexagonal structure is particularly stable for both Si and Ge.

DOI: 10.1103/PhysRevLett.95.115502 PACS numbers: 61.46.+w, 68.65.−k

Semiconductor nanowires with diameters of a few nanometers can be grown nowadays by vapor-liquid-solid [1], solution-growth [2], or oxide-assisted growth methods [3]. These nanowires usually depict a crystalline core surrounded by an oxide outer layer. Further removal of the oxide layer by acid treatment may lead to hydrogen-passivated Si nanowires as thin as 1 nm [3]. Pristine (nonpassivated) Si wires with diameters of a few nanometers have also been produced from Si vapor deposited on graphite [4]. The elongated shape of Si and Ge clusters of up to a few tens of atoms, determined by mobility measurements [5], indicates that even thinner (with diameters smaller than 1 nm) pristine structures can been produced.

The growth of such small-diameter structures raises the question of the limit of a bulklike description of bonding in these nanowires, since for small enough diameters, the predominance of surface atoms over inner (bulklike) atoms will eventually lead to bonds (and structures) distinct from those of the bulk system. In the present work, we use first-principles calculations to investigate several periodic structures of pristine Si and Ge nanowires of infinite length, with diameters ranging from 0.4 to 2.0 nm. (Here, the nanowire diameter D is defined as that of the smallest cylinder that contains the wire.)

Our calculations are performed in the framework of Kohn-Sham density functional theory (DFT) [6], within the generalized-gradient approximation (GGA) [7] and norm-conserving pseudopotentials [8] in the Kleinman-Bylander factorized form [9]. We use the LCAO method implemented in the SIESTA code [10], with a double-zeta basis set plus polarization orbitals. Total-energy differences are converged to within 10 meV/atom with respect to calculational parameters [11]. An order-N density-matrix tight-binding [12] methodology (DMTB) is used to study the energetics of larger structures.

The majority of the nanowire structures we consider in this work are derived from crystalline structures. As a first test of the methodology, we compute the total energy per atom $E_{\rm tot}$, at zero pressure, for the following bulk phases: cubic diamond (cd), hexagonal diamond (hd), β-tin, simple hexagonal (sh), simple cubic (sc), bcc, hcp, and fcc. In Table I, we show the total energy per atom of each structure, $\Delta E_{\rm tot} = E_{\rm tot} - E_{\rm tot}^{\rm cd}$, relative to the total energy of the cd phase $E_{\rm tot}^{\rm cd}$. We observe that $\Delta E_{\rm tot}$ is within 0.20–0.40 eV/atom for the sc, sh, and β-tin phases, for both Si and Ge. Our $\Delta E_{\rm tot}$ results for the sc, sh, and β-tin phases of Si, and for the β-tin phase of Ge are in good agreement with recent GGA calculations [13]. Our calculated results for the diamond to β-tin transition pressure for Si (109 kbar) and Ge (92 kbar) are also in good agreement with experimental results and previous GGA calculations [13,14].

Next, we address the structure and *ab initio* energetics of several stable geometries of Si and Ge nanowires with diameters between 0.4 and 2.0 nm. We start with a description of the three classes of structures we consider:

Diamond-structure nanowires.—Structures in this class are derived from the cd bulk phase, with the nanowire axis oriented along the (100) and (110) directions. The latter is the observed orientation of Si nanowires with diameters between 3 and 10 nm [15]. We considered several nanowires in the 0.4 nm $< D <$ 2.0 nm range. These structures are obtained from the cd bulk by defining the wire axis along the indicated crystalline direction and including atoms that fall within a specified distance from the axis. Low-coordinated surface atoms are removed. For both Si and Ge, only the wires with $D > 1$ nm, oriented along (110), remain cd-like after the *ab initio* geometry optimi-

TABLE I. Calculated total energies per atom $\Delta E_{\rm tot}$, in eV/atom, of selected Si and Ge bulk phases, relative to the cubic diamond phase.

	hd	β-tin	sh	sc	bcc	hcp	fcc
Si	0.01	0.31	0.33	0.36	0.52	0.52	0.55
Ge	0.02	0.23	0.24	0.23	0.30	0.29	0.29

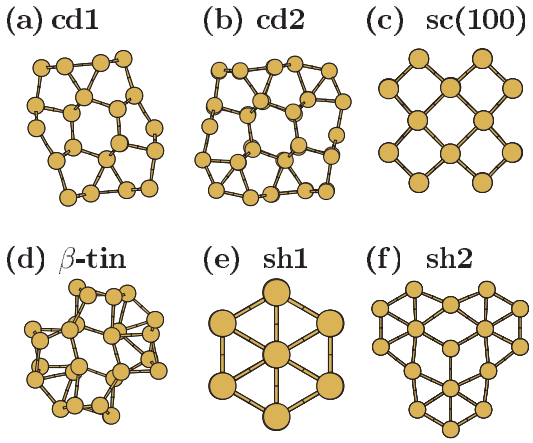

FIG. 1 (color online). Cross sections of selected Ge nanowire structures labeled according to the parent bulk phase. In (a) and (b), wires derived from the cubic diamond structure, with axis along the (110) direction; in (c), a simple cubic wire; in (d), a β-tin wire with axis along the bulk c direction; in (e) and (f), simple hexagonal wires with axis along the bulk c direction.

zation. The geometries of two of these wires, labeled cd1 and cd2, are shown in Figs. 1(a) and 1(b), respectively, for the case of Ge. The corresponding structures for Si are very similar. Both wires undergo reconstruction at the surface but retain a crystalline core at the central interstitial channel, as shown in the Figure. The cd wires with $D < 1$ nm undergo extensive reconstruction towards amorphouslike structures. Below, we comment on the particular case of the (100)-oriented wire shown in Fig. 2(a) ($D \sim 0.9$ nm), which becomes very corrugated after reconstruction, displaying pentagonal rings at the surface.

Fullerenelike nanowires.—The second class of structures derives from fullerenelike geometries [4,16]. We consider the two fullerene-based geometries proposed in Ref. [4], namely, the Si_{20} cage polymer (ful1) and the Si_{24} cage polymer (ful2). Based on the predicted stability of filled-fullerenelike clusters [16]; we also consider variations of these nanowires, labeled f-ful1 and f-ful2, where two extra atoms are included inside the cage. f-ful2 is shown in Fig. 2(b). Its corrugated structure, with the presence of fivefold rings at the surface, is similar to that of the

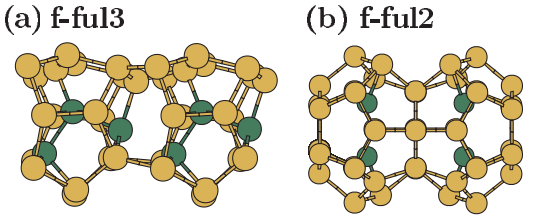

FIG. 2 (color online). Side view of corrugated Ge nanowire structures. In (a), corrugated wire resulting from a structural instability of a (100) cubic diamond nanowire; in (b), a filled-fullerene nanowire. Inner atoms are shown as green spheres.

wire which results from the reconstruction of the cd(100) wire, shown in Fig. 2(a). For this reason, we classify the latter as fullerenelike, and label it f-ful3. We have also investigated filled-fullerenelike nanowires of smaller diameters, based on Si_{12} and Si_{16} cages, with one additional atom in the center of the cage.

High-density nanowires.—Structures in this class are derived from the high-density β-tin, sc, and sh bulk phases. The simple cubic (sc) Ge nanowire oriented along the (100) direction is shown in Fig. 1(c). It shows very few distortions relative to the bulk structure, and its energy is lower than that of the sc structures oriented along (110) and (111) directions. The β-tin nanowire has its axis parallel to the bulk c axis, passing through the center of an interstitial channel. While the initial geometry of this wire is somewhat similar to that of the sc nanowire, the corresponding relaxed geometries shown in Figs. 1(c) and 1(d) are very different, due to the substantial relaxation of the β-tin geometry. All sh nanowires oriented along the bulk c direction retain the crystalline order along the wire axis after geometry optimization, regardless of the wire radius. Two of these, the sh1 and sh2 structures, are shown in Figs. 1(e) and 1(f), respectively. The sh structure oriented along the $(10\bar{1}0)$, with $D \sim 0.8$ nm, has a much higher formation energy than any of those oriented along the c axis. An empty-hexagon variation of sh1 is also considered, where the atom at the hexagon center is removed. Overall, for all structures in the above three classes, the relaxed Si nanowires are structurally very similar to the Ge ones.

The calculated total energies of the Ge nanowires are shown in Fig. 3 (we show only geometries with $D <$ 1.4 nm), where we plot ΔE_{tot} (relative to the cd bulk phase, as defined previously) as a function of D. The corresponding results for Si are very similar. We observe that in the 0.9 nm $< D <$ 1.4 nm range, the formation energies of the high-density sc, sh, and β-tin nanowires, and also of the fullerenelike wires, are very close to the energies of cd1

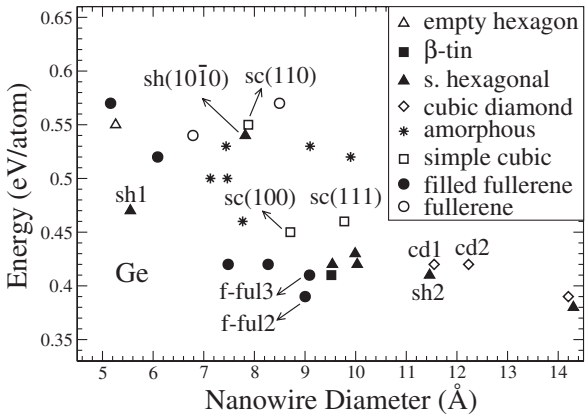

FIG. 3. First-principles total energies (in eV/atom), relative to cd bulk energy, of Ge nanowires as a function of nanowire diameter. Labeling of the structures is explained in the text.

and cd2, with energy differences of ~0.05 eV/atom or less. Note that these values are 1 order of magnitude smaller than the energy differences of the corresponding bulk phases in Table I. This shows that the energetics of wire formation, at such small diameters, is strongly affected by surface effects [17].

Figure 3 also shows that the amorphous wires, derived from the instabilities of thin cd wires, have higher formation energies than the high-density and the fullerenelike wires of comparable diameters. This suggests that amorphous wires in this diameter range could only be produced in conditions very far from thermodynamical equilibrium. As expected, hollow geometries like the unfilled-fullerene and the empty-hexagon structures also have very high energies, when compared to the denser structures. Figure 3 also shows that among the nanowires with $D < 0.7$ nm, the sh1 structure appears below and to the left in the energy vs diameter diagram, which suggests a high stability for this structure when compared to the other small-diameter geometries. In the range $0.7\ \text{nm} < D < 0.9$ nm, filled-fullerenelike wires are the most stable ones.

The results above suggest that the energetics of nanowire formation is determined by the interplay between the energies of a bulk part and a surface part of the wire. To investigate that aspect in more detail, we choose cd- and sh-based Si and Ge nanowires for a comparative study, including additional *ab initio* calculations for larger cd ($D \sim 2$ nm) and sh ($D \sim 1.5$ nm) structures. In Fig. 4, we show ΔE_{tot} for the cd and sh Si wires, respectively, as a function of the inverse nanowire diameter D^{-1}. We also include explicitly in the figure the ΔE_{tot} values of the respective bulk phases, which correspond to $D^{-1} = 0$. The figure shows distinct trends for the cd- and sh-based Si nanowires, with a much larger variation of the total energy per atom as a function of D^{-1} for the cd-based wires than for the sh-based ones. Moreover, the energies of the two types of Si nanowires are very close for $D \sim 1.2$ nm ($D \sim 1.4$ nm for Ge).

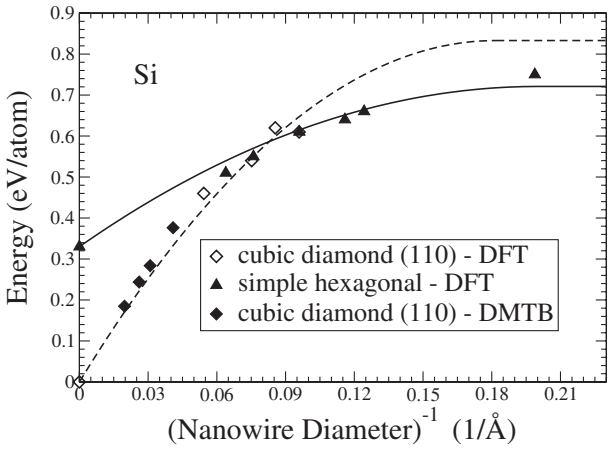

FIG. 4. First-principles (DFT) and tight-binding (DMTB) total energies (in eV/atom), relative to the cd bulk energy, of Si nanowires as a function of the inverse of the nanowire diameter. The dashed (solid) line shows the curve obtained from a continuum model (see text), parameterized for cd (sh) wires.

The results of the first-principles calculations shown in Fig. 4 are reasonably well fitted by the expression

$$\varepsilon_{\text{nw}} = \varepsilon_s + (\varepsilon_b - \varepsilon_s)\frac{(D - 2\rho^{-1/3})^2}{D^2} \qquad (1)$$

In Eq. (1), ε_{nw} is ΔE_{tot} for the nanowire based on a given structure (cd or sh), while ε_b and ρ are, respectively, ΔE_{tot} and the number of atoms per volume for the corresponding bulk structure. ε_s is a measure of the surface energy per atom of the nanowire. ε_b and ρ are obtained from the bulk first-principles calculations, leaving ε_s as the only fitting parameter. In Fig. 4 we plot Eq. (1) with $\varepsilon_s = 0.83$ eV for the cd structure and $\varepsilon_s = 0.72$ eV for the sh structure. An equally good fitting is obtained for Ge wires, with $\varepsilon_s = 0.58$ eV for cd and $\varepsilon_s = 0.47$ eV for sh. (For both Si and Ge, the fitting includes the *ab initio* energies for the larger structures not shown in Fig. 3.)

Equation (1) results from a simple continuum model where we consider a cylindrical nanowire with diameter D, density ρ, and total energy E_{nw}. By decomposing E_{nw} into contributions due to the bulklike atoms and to the low-coordinated surface atoms, we write $E_{\text{nw}} = \varepsilon_b \rho V_b + \varepsilon_s \rho V_s$. By considering a surface thickness of $\rho^{-1/3}$, we obtain Eq. (1).

Although this continuum model would be strictly valid only in the limit $D^{-1} \to 0$, it provides a simple interpretation for the larger variation of ε_{nw} as a function of D^{-1} for the cd-based wires when compared with the sh-based ones. In Eq. (1), the variation of ε_{nw} with D is proportional to $\Delta\varepsilon = \varepsilon_s - \varepsilon_b$. $\Delta\varepsilon$ is about twice as large for the cd phase than for the sh phase for both Si and Ge, which means that the energy cost of a cd surface is much larger than that of a sh surface. This arises from the fact that surface atoms in a cd structure are undercoordinated (coordination three or less), while the surface atoms in a sh structure are still highly coordinated, which reduces the energy cost of its surface. It is interesting to point out that our one-parameter continuum model, least-square fitted to four (six) points for the cd (sh) geometries, displays a crossing between the two curves for $D \sim 1.2$ nm. Hence, the model suggests a stability inversion resulting essentially from the larger $\Delta\varepsilon$ for the cd phase. The same stability inversion is indicated by the very close *ab initio* values we obtain for ε_{nw} for the sh- and cd-based wires, for $D \sim 1.2$ nm. Moreover, it is interesting to notice that the structural ''transition'' of the cd class of nanowires suggested by the first-principles results, from crystallinelike (for $D > 1$ nm) to amorphouslike (for $D < 1$ nm), occurs at diameters which are very near the cd-sh stability inversion.

To verify the applicability of Eq. (1) to wires of larger radii, we have performed DMTB calculations for thicker cd Si wires. The results for (110)-oriented wires with

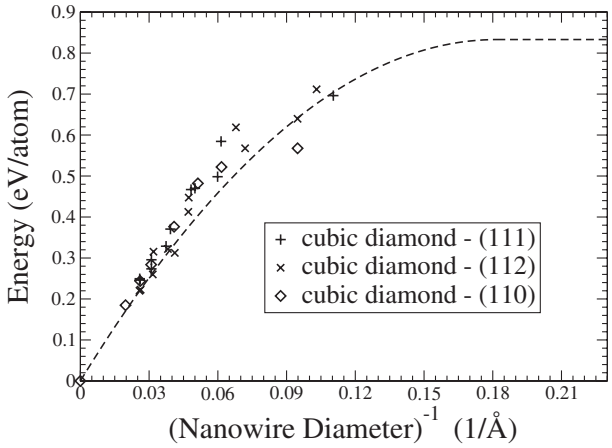

FIG. 5. Tight-binding energies (in eV/atom), of cd Si nanowires oriented along (111), (112), and (110) directions, as a function of inverse nanowire diameter. The dashed line corresponds to a continuum model (see text) parametrized as in Fig. 4.

2 nm $> D >$ 5 nm are included in Fig. 4 [but not in the fitting of Eq. (1)]. The agreement between the *ab initio*-fitted Eq. (1) and the DMTB values for $\varepsilon_{\mathrm{nw}}$ is very good, at larger diameters. We also consider wires oriented along the (111) and (112) directions. The DMTB results are shown in Fig. 5, superimposed with the same first-principles parameterization of Eq. (1) as in Fig. 4. Figure 5 shows that the DMTB results follow the trend of Eq. (1), with variations in energy of the order of $\sim$0.1 eV/atom due to wire structure and orientation. An important point emerges from this figure: surface energies of cd wires, in the diameter range considered, are similar for different orientations (more accurately so for $D > 2$ nm), and are reasonably well described by an average surface energy (our $\Delta\varepsilon$) which measures the average subcoordination of the surface, as discussed above. Moreover, Fig. 5 suggests that the cd wires in the (110) orientation should have lower energies in the diameter range of the stability inversion indicated by the first-principles results.

Finally, let us comment on the stability of the filled-fullerene and sh1 structures for very small diameters. Although Eq. (1) cannot be applied to the filled-fullerene geometries (there is no bulk structure associated with them), the calculated energies behave as a decreasing function of the diameter. A hypothetical curve for these structures would cross that of $\varepsilon_{\mathrm{nw}}$ for the sh phase for $D \sim$ 0.7 nm, as can be seen in Fig. 3. This is consistent with the special stability of sh1 for very small diameters, and it suggests that the sh phase might be the stable one for ultrathin nanowires.

In summary, our calculations indicate a transition from sp^3-based Si and Ge nanowire geometries to structures based on denser bulk phases and fullerenelike structures, for diameters smaller than $\sim$1.2 nm for Si and $\sim$1.4 nm for Ge. Diamond-structure geometries are unstable against distortion towards amorphouslike wires, for diameters smaller than 1 nm. We also introduce a class of filled-fullerene wires that are the most stable for diameters between 0.8 and 1 nm. Last, for very thin wires ($D \sim$ 0.5 nm), we find that a simple hexagonal structure is particularly stable for both Si and Ge.

We acknowledge support from the Brazilian agencies CNPq, FAPEMIG, and Instituto do Milênio em Nanociências-MCT.

*Electronic address: chacham@fisica.ufmg.br

[1] A. M. Morales and C. M. Lieber, Science **279**, 208 (1998); H. Z. Zhang *et al.*, Appl. Phys. Lett. **73**, 3396 (1998).
[2] J. D. Holmes *et al.*, Science **287**, 1471 (2000).
[3] D. D. D. Ma *et al.*, Science **299**, 1874 (2003).
[4] Bjorn Marsen and Klaus Sattler, Phys. Rev. B **60**, 11 593 (1999).
[5] M. F. Jarrold and V. A. Constant, Phys. Rev. Lett. **67**, 2994 (1991); J. M. Hunter *et al.*, Phys. Rev. Lett. **73**, 2063 (1994).
[6] W. Kohn and L. J. Sham, Phys. Rev. **140**, A1133 (1965).
[7] J. P. Perdew, K. Burke, and M. Ernzerhof, Phys. Rev. Lett. **77**, 3865 (1996).
[8] N. Troullier and J. L. Martins, Phys. Rev. B **43**, 1993 (1991).
[9] L. Kleinman and D. M. Bylander, Phys. Rev. Lett. **48**, 1425 (1982); X. Gonze, R. Stumpf, and M. Scheffler, Phys. Rev. B **44**, 8503 (1991).
[10] P. Ordejón, E. Artacho, and J. M. Soler, Phys. Rev. B **53**, R10 441 (1996); D. Sánchez-Portal *et al.*, Int. J. Quantum Chem. **65**, 453 (1997).
[11] We use the following parameters: energy shifts [10] of 0.01 Ry for cd, hd, β-tin, sc, and sh (bulk and nanowires); and 0.0001 Ry for bulk bcc, hcp, and fcc. Mesh cutoffs of 400 Ry (Si) and 300 Ry (Ge) for the **k**-space expansion of the charge density. 1000–7000 **k** points for bulk calculations; and 3–5 **k** points (along the nanowire axis) for nanowires. Residual forces are less than 0.04 eV/Å for all optimized geometries. For nanowire calculations, supercell dimensions in directions perpendicular to the wire axis ranged from 15 to 32 Å, with vacuum regions of 10 Å.
[12] X.-P. Li, R. W. Nunes, and D. Vanderbilt, Phys. Rev. B **47**, 10 891 (1993); I. Kwon *et al.*, Phys. Rev. B **49**, 7242 (1994).
[13] N. Moll *et al.*, Phys. Rev. B **52**, 2550 (1995); I. H. Lee and R. M. Martin, Phys. Rev. B **56**, 7197 (1997); C. Cheng, Phys. Rev. B **67**, 134109 (2003).
[14] A. Mujica *et al.*, Rev. Mod. Phys. **75**, 863 (2003), and references therein; K. Gaál-Nagy, P. Pavone, and D. Strauch, Phys. Rev. B **69**, 134112 (2004).
[15] Y. Wu *et al.*, Nano Lett. **4**, 433 (2004).
[16] Uzi Landman *et al.*, Phys. Rev. Lett. **85**, 1958 (2000); U. Röthlisberger, W. Andreoni, and M. Parrinello, Phys. Rev. Lett. **72**, 665 (1994).
[17] Y. Zhao and B. I. Yakobson, Phys. Rev. Lett. **91**, 035501 (2003).